Original Article

Phytochemical screening of bioactive compounds and antioxidant activity of methanol extract from *Melia Azedarach* L. fruit: Exploring for antidiabetic potential

Qurratu Aini[1], Nurdin Nurdin[2*], Mustanir Mustanir[3], Safrida Safrida[4] and Tio R. Fauzi[5]

[1]Graduate School of Mathematics and Applied Sciences, Universitas Syiah Kuala, Banda Aceh, Indonesia; [2]Department of Biology, Faculty of Islamic Studies, Universitas Muhammadiyah Aceh, Banda Aceh, Indonesia; [3]Department of Chemistry, Faculty of Mathematics and Natural Sciences, Universitas Syiah Kuala, Banda Aceh Indonesia; [4]Department of Biology Education, Faculty of Teacher Training and Natural Sciences, Universitas Syiah Kuala, Banda Aceh, Indonesia; [5]Pharmacy Study Program, Faculty of Medicine and Health Sciences, Universitas Islam Negeri Maulana Malik Ibrahin Malang, Malang, Indonesia

*Corresponding author: nurdin@usk.ac.id

Abstract

Melia azedarach L. (neem fruit) is a traditional plant with diverse bioactive constituents, yet its phytochemical profile and pharmacological potential remain underexplored. This study aimed to screen bioactive compounds and evaluate the antioxidant activity of methanol extract from *M. azedarach* fruit, while further performing computational exploration on its antidiabetic potential. *M. azedarach* fruits were macerated in methanol and analyzed through phytochemical screening, total phenolic content (TPC), total flavonoid content (TFC), and antioxidant activity (DPPH assay). GC-MS was used to identify chemical constituents. Molecular docking was performed using a blind docking approach in CBDock2 against five protein targets, which included DPP-4, PTPN1, α-amylase, NrfA, and AKR1B1. Protocol validation was ensured by successful re-docking of co-crystallized ligands (RMSD <2.0 Å). The extract was observed to contain terpenoids, steroids, flavonoids, and phenolics, with high TPC (479.8 mg GAE/g) and TFC (52.7 mg QE/g). Antioxidant activity was moderate (IC_{50}=102.27 µg/mL). GC-MS identified 14 compounds, including cucurbitacins, ursolic acid derivatives, α-amyrin, taraxasterol, and ergostane-type sterols. Docking revealed moderate affinities (–5.0 to –6.5 kcal·mol^{-1}) for most compounds. The cucurbitacin bound α-amylase (–13.6 kcal·mol^{-1}) and NrfA (–8.5 kcal·mol^{-1}), and taraxasterol exhibited broad-spectrum activity across all targets (–7.1 to –9.2 kcal·mol^{-1}). *M. azedarach* fruit demonstrates moderate antioxidant activity and contains diverse phytochemicals with multitarget interactions relevant to glucose regulation. Strong binding to DPP-4, PTPN1, α-amylase, and AKR1B1 suggests potential antidiabetic properties through inhibition of carbohydrate digestion, enhancement of insulin signaling, and prevention of diabetic complications.

Keywords: Cucurbitacins, diabetes mellitus, DPPH, neem fruit, taraxasterol

Introduction

Indonesia is a megadiverse country with abundant medicinal plants that have long been used in traditional health practices [1]. In Aceh, *Melia azedarach* L. (family Meliaceae), locally known as *boh putek uteun*, is one of the plants widely applied in community medicine [2,3]. The fruit is traditionally used to treat various ailments, including cancer, cardiovascular disorders, high cholesterol, and, notably, diabetes mellitus [4-6]. This long-standing ethnomedicinal use suggests the presence of bioactive compounds that may target pathways relevant to metabolic diseases.

Received: August 13, 2025 - Accepted: September 17, 2025 - Published online: September 19, 2025

Diabetes mellitus is a chronic metabolic disorder characterized by hyperglycemia resulting from impaired insulin secretion, insulin resistance, or both. In 2021, an estimated 529 million people were living with diabetes worldwide, with prevalence projected to rise to more than 1.3 billion by 2050 [7]. This situation underscores the urgent need for affordable natural products with multitarget actions to support diabetes management. To address that, previous studies on *M. azedarach* leaves and twigs have identified diverse phytochemicals, including flavonoids, terpenoids, steroids, phenols, and saponins, with documented antibacterial, antioxidant, and antidiabetic properties [6,8,9]. In Ethiopian traditional medicine, *M. azedarach* extracts are used to manage diabetes, and experimental studies confirmed that leaf extracts reduced plasma glucose and insulin levels while improving glucose tolerance [10]. These effects were attributed to a multitarget mechanism, including enhanced insulin sensitivity and delayed gastric emptying [10]. Similarly, in an acute diabetic rat model, a study reported that ethanol extracts of *M. azedarach* reduced blood glucose by 14.8%, supporting its in vivo antidiabetic efficacy [11].

To further explore possible mechanisms underlying the antidiabetic potential of *M. azedarach*, molecular docking was conducted against key protein targets involved in glucose regulation and diabetic complications. Dipeptidyl Peptidase-4 (DPP-4) plays a central role in glucose homeostasis by degrading incretin hormones, and its inhibition is a well-established strategy to prolong insulin secretion and lower blood glucose [12]. Protein Tyrosine Phosphatase 1B (PTPN1) acts as a negative regulator of insulin receptor signaling; therefore, its inhibition enhances insulin sensitivity and glucose uptake in peripheral tissues [13,14]. In addition, α-amylase is a major digestive enzyme responsible for breaking down dietary starch into glucose, and blocking this enzyme can slow carbohydrate absorption and reduce postprandial hyperglycemia [15,16]. Beyond glucose metabolism, oxidative stress contributes significantly to diabetes pathophysiology. For this reason, NADH-quinone oxidoreductase (NrfA), a redox-related enzyme, was included as a target to evaluate potential antioxidant-mediated protective effects [17]. Finally, Aldose Reductase (AKR1B1) is a key enzyme in the polyol pathway whose hyperactivity under hyperglycemic conditions contributes to complications such as neuropathy, retinopathy, and nephropathy [18,19]; its inhibition is therefore considered protective against long-term diabetic damage.

Despite existing evidence, the fruit of *M. azedarach* remains underexplored, particularly in relation to its phytochemical profile and potential antidiabetic activity. Given its traditional use in Aceh for diabetes treatment, systematic evaluation of the fruit is warranted. Hence, this study was designed to conduct phytochemical screening, quantify total phenolic and flavonoid contents, and evaluate antioxidant activity of methanol fruit extracts. In addition, Gas Chromatography–Mass Spectrometry (GC-MS) was employed to characterize the chemical constituents, and molecular docking was performed against DPP-4, PTPN1, α-amylase, NrfA, and AKR1B1 to explore the antidiabetic potential of the identified compounds.

Methods

Sample collection, preparation, and extraction

Melia azedarach L. fruits were collected from the Gampong Teu Dayah area, Kuta Malaka District, Aceh Besar Regency. Plant identification and classification were confirmed at the Biology Laboratory, Faculty of Mathematics and Natural Sciences, Universitas Syiah Kuala. The extraction was then performed per the suggestion of a previous literature [20]. Approximately 3 kg of fresh fruit was cleaned under running water to remove adhering dirt, then air-dried at ambient temperature without direct sunlight exposure. The dried samples were ground using a blender to obtain coarse fruit powder, which was subsequently weighed. The powdered material was macerated in methanol for 72 hours at room temperature (25 °C). The macerates were filtered, and the resulting filtrate was concentrated under reduced pressure using a rotary evaporator to obtain the methanol extract of *M. azedarach* fruit.

Qualitative phytochemical analysis

The methanol extract of *M. azedarach* L. fruit was subjected to phytochemical analysis to identify secondary metabolite components, following the recommendation of previous literature [20,21].

Phenolic compounds were tested by dissolving 20 mg of extract in methanol and adding five drops of 5% $FeCl_3$. A blackish-blue color indicated the presence of phenolic compounds (tannins). Flavonoids were detected using the Shinoda test, where 50 mg of extract dissolved in methanol was mixed with 0.5 g of Mg powder and 0.5 mL of concentrated HCl. A red or purplish color confirmed the presence of flavonoids. Saponins were detected by dissolving 50 mg of extract in methanol, adding 5 mL of distilled water, and shaking vigorously. The formation of stable foam lasting for 30 minutes indicated a positive result. Steroids and terpenoids were detected by dissolving the extract in methanol, followed by the addition of Liebermann–Burchard (LB) reagent; a green or blue color indicated steroids, while red or purple indicated terpenoids. Alkaloids were detected by dissolving 100 mg of extract in 3 mL of methanol, followed by the addition of 2 mL NH_3 and 5 mL chloroform. The filtrate was collected and treated with 5% HCl (5 mL) to form two layers. The upper layer was separated and divided into three tubes, to which Mayer, Wagner, and Dragendorff reagents were added. The appearance of white, yellow, and reddish-brown precipitates indicated a positive alkaloid test.

Quantification of total phenolic content

Total phenolic content (TPC) in the extract was measured using the Folin–Ciocalteu method, following the recommendation of a previous study [22]. A 5 mg extract sample was dissolved in distilled water to a final volume of 5 mL. From this, 0.2 mL was mixed with 15.8 mL distilled water and 1 mL Folin–Ciocalteu reagent. After 5 minutes, 3 mL of 10% Na_2CO_3 solution was added, and the mixture was incubated for 120 minutes at room temperature (25 °C). Absorbance was measured at 765 nm using a UV-Vis spectrophotometer (Shimadzu UVmini-1240, Kyoto, Japan). A standard calibration curve was prepared using gallic acid. A stock solution of 5 mg gallic acid was dissolved in 10 mL distilled water, and aliquots of 1.0, 1.25, 1.5, 1.75, and 2.0 mL were diluted to 5 mL to obtain concentrations of 100, 125, 150, 175, and 200 µg/mL. Each standard was processed in the same way as the samples, and absorbance was measured at 765 nm. TPC was expressed as milligrams of gallic acid equivalents per gram of extract (mg GAE/g).

Quantification of total flavonoid content

Total flavonoid content (TFC) of the *M. azedarach* extract was determined using the aluminum chloride colorimetric method, following the protocol previously described with minor modifications [23]. Briefly, 5 mg of dry extract was dissolved in 5 mL of methanol. From this, 1 mL was mixed with 0.2 mL of 10% $AlCl_3$ solution, 0.2 mL of 1 M potassium acetate, 3 mL methanol, and 5.6 mL distilled water. The mixture was incubated for 10 minutes at room temperature (25 °C). For standard preparation, 5 mg of quercetin was dissolved in 10 mL of methanol to obtain the stock solution. Aliquots of 200, 400, 600, 800, and 1000 µL were diluted to 5 mL with methanol to yield concentrations of 20, 40, 60, 80, and 100 µg/mL, respectively. Each standard solution (1 mL) was treated with the same reagents as the samples and incubated for 30 minutes at room temperature (25 °C). Absorbance was measured at 440 nm using a UV-Vis spectrophotometer (Shimadzu UVmini-1240, Kyoto, Japan). TFC was expressed as milligrams of quercetin equivalent per gram of extract (mg QE/g).

DPPH antioxidant activity test

The antioxidant activity of the methanol extract of *Melia azedarach* fruit was evaluated using the DPPH free radical scavenging method, following the procedure described previously with slight modifications [24]. Briefly, 2.5 mg of extract was dissolved in methanol and diluted to 5 mL, then serially prepared to concentrations of 6.25, 12.5, 25, 50, and 100 µg/mL. For each concentration, 4 mL of the extract solution was mixed with 1 mL of DPPH solution (7.9 mg DPPH dissolved in methanol up to 50 mL; molecular weight 394.32 g/mol; absorbance 0.75–0.98). The mixtures were homogenized and incubated in the dark at 37 °C for 30 minutes. Absorbance was measured at 517 nm using a UV-Vis spectrophotometer, with methanol as the blank. Ascorbic acid was used as a positive control at concentrations of 3, 6, 9, 12, and 15 µg/mL, prepared and analyzed using the same procedure. The percentage inhibition of DPPH radicals was calculated, and IC_{50} values (concentration required to inhibit 50% of DPPH radicals) were determined for both the extract and the standard.

Gas chromatography-mass spectrometry (GC-MS) analysis

GC-MS analysis was carried out using an AS 2000 autosampler coupled to a mass spectrometer, adjusted according to the manufacturer's recommendations. A 1 µL sample was injected using the hot-needle technique with a split ratio of 25:1. Separation was performed on a 30 m SPB-50 column (0.25 mm i.d., 0.25 µm film thickness; Supelco, Bellefonte, PA, USA). The injector temperature was maintained at 230 °C, the interface at 250 °C, and the ion source at 200 °C. Helium was used as the carrier gas at a constant flow rate of 1 mL/min.

The oven temperature program began with an initial isothermal step at 70 °C for 5 minutes, followed by a ramp of 5 °C/min to 310 °C, where it was held for 1 minute. The system was then equilibrated at 70 °C for 6 minutes before the next injection. Mass spectra were acquired at two scans per second over a mass range of m/z 50–600. Chromatograms and mass spectra were processed using MASSLAB software (Thermo Quest, Manchester, UK). Retention times and spectral data were compared against the MASSLAB database, and compound identification was performed using the PubChem database.

ADMET Profiling

Compounds identified from the *M. azedarach* extract based on the GC-MS analysis were retrieved from PubChem in SDF format. Absorption, Distribution, Metabolism, Excretion, and Toxicity (ADMET) parameters were predicted using the DeepPK platform (Biosig Lab). The evaluated parameters included Caco-2 permeability, human intestinal absorption (HIA), bioavailability probability (F20), plasma protein binding (PPB), volume of distribution (Vd/VDss), CYP2C9 inhibition, CYP3A4 substrate prediction, clearance, and half-life. Toxicological parameters included Ames test (mutagenicity), carcinogenicity, and maximum tolerated concentration (MTC). All results presented in the ADMET table were generated directly from the DeepPK output without manual modification.

Molecular Docking

Molecular docking was performed using a blind docking approach with CBDock2. The crystal structures of the selected target proteins were retrieved from the RCSB Protein Data Bank (accessed July 15, 2025): 2P8S (DPP-4), 2QBP (PTPN1), 2QV4 (α-amylase), 3TOR (NrfA), and 4JIR (AKR1B1). All chains in each PDB file were retained to allow unbiased cavity detection, and the protein structures were used in their original form without chain deletion or additional refinement. Ligand structures corresponding to the identified compounds were retrieved from PubChem as canonical SMILES and converted into 3D SDF files prior to docking.

Validation of the docking protocol was conducted by re-docking the co-crystallized ligands into their respective protein binding sites using the same parameters applied to the GC-MS-identified ligands. The protocol was considered valid when the root-mean-square deviation (RMSD) between the re-docked and crystallographic ligand poses was <2.0 Å, calculated in PyMOL by fitting the heavy atoms of the ligands (**Table 1**).

Table 1. Redocking validation and grid box parameters for the protein-ligand docking simulations

PDB ID	RMSD (Å)	Grid size			Grid position (Å)		
		X	Y	Z	X	Y	Z
2P8S	1.5807	16	10	10	41.367	51.401	36.442
2QBP	1.0652	16	20	10	48.323	9.607	3.650
2QV4	1.8430	16	20	10	12.942	47.169	50,704
3TOP	1.9417	8	14	14	−31.425	35.7	26.2
4JIR	0.5581	6	8	6	−5.773	8.521	17.888

RMSD: root-mean-square deviation

Blind docking was performed on the CBDock2 server using default cavity detection and search parameters. Side-chain flexibility was enabled for residues within the predicted binding pockets to improve accommodation of ligand interactions. For each protein–ligand pair, poses were ranked by predicted binding energy (kcal/mol), and the top-scoring pose (lowest binding energy) was selected for further analysis. Docking simulations were executed on September 10, 2025. The selected protein–ligand complexes were imported into BIOVIA Discovery Studio Visualizer (v24.1.0) for interaction analysis. Two-dimensional diagrams highlighting hydrogen

bonds and hydrophobic contacts were generated. Binding energies (kcal/mol) and key interacting residues for each complex were recorded and reported.

Results

Phytochemical groups

Results from the qualitative phytochemical screening of the methanol extract of *M. azedarach* fruit are presented in **Table 2**. Flavonoids were confirmed by the formation of an orange color in the Shinoda test, while phenolic compounds gave a dark black coloration with ferric chloride, indicating a positive reaction. The Liebermann–Burchard test produced a moss-green color, confirming the presence of steroids, whereas a pink color change indicated terpenoids. In contrast, saponins were not detected, as no persistent foam was observed during the frothing test. Similarly, alkaloid screening was negative for all three reagents: Mayer's reagent did not yield white precipitates, Wagner's reagent showed no brown sediment, and Dragendorff's reagent did not produce brick-red deposits. These results suggest that the methanol extract of *M. azedarach* fruit is rich in phenolics, flavonoids, terpenoids, and steroids, but lacks detectable levels of saponins and alkaloids.

In the quantitative analysis, we found that the TP of the extract was 479.8 mg GAE/g, while the TFC was 52.7 mg QE/g. The phenolic concentration was markedly higher than that of flavonoids, indicating that phenolics represent the dominant secondary metabolites in the extract.

Table 2. Phytochemical test results of methanol extractfruit M. Azedarach L.

Compound groups	Results	Information
Flavonoids	Positive	Orange color formed
Phenolics	Positive	Dark black color formed
Saponins	Negative	Does not produce foam
Terpenoids	Positive	Pink color formed
Steroids	Positive	Moss green color is formed
Alkaloids		
Mayer's reagent	Negative	Does not produce white deposits
Wagner's reagent	Negative	Does not produce brown sediment
Dragendorff's reagent	Negative	Does not produce brick red precipitate

DPPH antioxidant activity

The antioxidant activity of the methanol extract of *M. azedarach* fruit was determined using the DPPH free radical scavenging assay. **Figure 1** presents the inhibition curves, with the linear regression used for IC_{50} calculation. The extract demonstrated a clear concentration-dependent effect, where increasing concentrations of the extract resulted in higher percentages of DPPH radical inhibition. From the regression analysis, the IC_{50} value of the methanol extract was determined to be 102.27 µg/mL.

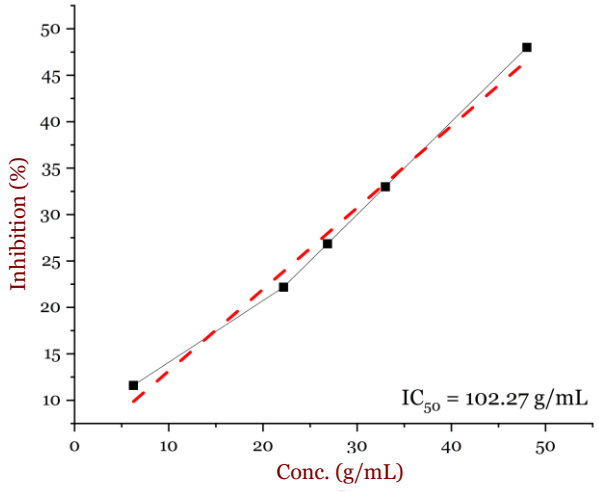

Figure 1. *M. azedarach* L. concentration-dependent inhibition of DPPH

Based on the classification proposed by Molyneux (2004), antioxidant capacity is categorized as strong (<50 µg/mL), moderate (100–150 µg/mL), or weak (>150 µg/mL). Accordingly, the methanol extract of *M. azedarach* fruit exhibited moderate antioxidant activity.

GC-MS-based identified phytoconstituents

The phytoconstituent profile of the methanol extract of *M. azedarach* fruit was analyzed using GC-MS. The chromatogram is presented in **Figure 2**, and the identified compounds are summarized in **Table 3**. The major constituents were fatty acids and their derivatives, along with several terpenoid and steroidal compounds. The most abundant compound was trans-13-octadecenoic acid (C6), which accounted for 55.35% of the total area, followed by linoleic acid (C5) at 19.11% and n-hexadecanoic acid (C2) at 8.71%. Other fatty acid derivatives such as octadecanoic acid (C7, 4.61%) and 6-octadecenoic acid (C10, 1.26%) were also detected, suggesting that long-chain fatty acids represent the predominant chemical class in the extract. In addition to fatty acids, the chromatogram revealed the presence of secondary metabolites with potential pharmacological importance. Notably, Himachal (C11, 4.72%), Cucurbitacin b, 25-desacetoxy- (C12, 0.53%), Taraxasterol (C13, 0.69%), and Stigmasta-3,5-diene (C14, 0.54%) were detected, which are classified as terpenoid and steroid compounds. Several minor components, including 3,5-octadien-2-ol (C1, 0.76%), 11,14-eicosadienoic acid methyl ester (C3, 0.47%), and 12-methyl-E,E-2,13-octadecadien-1-ol (C8, 0.49%), were also identified.

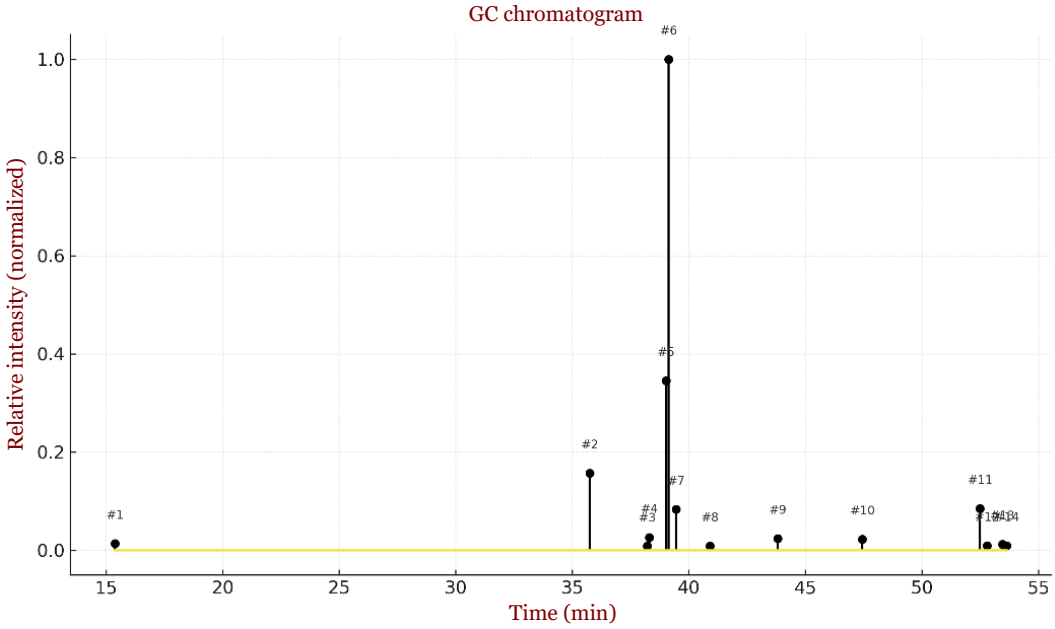

Figure 2. GC–MS chromatogram results of the methanol extract of *Melia azedarach* L. fruit showing 14 resolved peaks. Peak numbering corresponds to retention times and relative peak areas (normalized to the largest peak, Peak #6 at 39.14 min, 55.35%).

ADMET profile

The ADMET profiling of compounds C1–C14 indicated favorable absorption and distribution characteristics across most candidates, as presented in **Table 4**. All compounds were predicted to be absorbed in the intestine, with high Human Intestinal Absorption (HIA) and Caco-2 permeability values ranging between −4.21 and −4.99. Probability of oral bioavailability (F20) varied widely, from low values such as C7 (0.149) to higher probabilities observed in C1 (0.819), C11 (0.838), and C14 (0.847). Plasma protein binding (PPB) was generally moderate, with the highest values found in C12 (96.78%) and C14 (78.94%), suggesting strong plasma retention. Volume of distribution (Vd) values ranged from 0.62 to 3.59 L/kg, with C3, C8, and C9 showing relatively higher tissue distribution.

Table 3. GC-MS-identified phytoconstituents of the methanol extract

Peak	Time (min)	Compound	Area (%)	SMILES	Label
#1	15.38	3,5-Octadien-2-ol	0.76	CC/C=C/C=C/C(C)O	C1
#2	35.75	n-Hexadecanoic acid	8.71	CCCCCCCCCCCCCCCC(=O)O	C2
#3	38.22	11,14-Eicosadienoic acid, methyl ester	0.47	CCCCC/C=C/C/C=C/CCCCCCCCCC(=O)OC	C3
#4	38.31	6-Octadecenoic acid, methyl ester, (Z)-	1.44	CCCCCCCCCCC/C=C\CCCCC(=O)OC	C4
#5	39.03	Linoleic acid	19.11	CCCCC/C=C\C/C=C\CCCCCCCC(=O)O	C5
#6	39.14	trans-13-Octadecenoic acid	55.35	CCCC/C=C/CCCCCCCCCCC(=O)O	C6
#7	39.46	Octadecanoic acid	4.61	CCCCCCCCCCCCCCCCCC(=O)O	C7
#8	40.91	12-Methyl-E,E-2,13-octadecadien-1-ol	0.49	CCCC/C=C/C(C)CCCCCCCC/C=C/CO	C8
#9	43.82	9,17-Octadecadienal, (Z)	1.33	C=CCCCCCC/C=C\CCCCCCCC=O	C9
#10	47.45	6-Octadecenoic acid	1.26	CCCCCCCCCCCC=CCCCCC(=O)O	C10
#11	52.50	Himachal	4.72	CC1CCCC(C2=CC(C[C@H]([C@@H]12)O)C)(C)C	C11
#12	52.80	Cucurbitacin b, 25-desacetoxy-	0.53	CC(C)/C=C/C(=O)C(C)(C1C(CC2(C1(CC(=O)C3(C2CC=C4C3CC(C(=O)C4(C)C)O)C)C)C)O)O	C12
#13	53.46	Taraxasterol	0.69	C[C@H]1[C@@H]2[C@H]3CC[C@@H]4[C@]5(CC[C@@H](C([C@@H]5CC[C@]4([C@@]3(CC[C@]2(CCC1=C)C)C)C)(C)C)O)C	C13
#14	53.65	Stigmasta-3,5-diene	0.54	CC[C@H](CC[C@@H](C)[C@H]1CC[C@@H]2[C@@]1(CC[C@H]3[C@H]2CC=C4[C@@]3(CCC=C4)C)C)C(C)C	C14

Table 4. ADMET screening results for the secondary metabolites of *Melia azedarach*

Compound	Caco2	F20	HIA	PPB	Vd	CYP2C9 Inhibitor	CYP3A4	Clearance	Half-life (h)	Ames Toxicity	Carcinogenicity	MTC
C1	-4.21	0.819	Absorbed	49.16	1.36	Non-Inhibitor	Non-Substrate	7.07	≥ 3	Safe	Toxic	1.19
C2	-4.83	0.206	Absorbed	42.74	0.62	Non-Inhibitor	Non-Substrate	-0.07	≥ 3	Safe	Safe	2.21
C3	-4.91	0.246	Absorbed	40.2	3.59	Non-Inhibitor	Non-Substrate	2.8	≥ 3	Safe	Safe	2.03
C4	-4.93	0.239	Absorbed	33.34	2.6	Non-Inhibitor	Non-Substrate	4.44	≥ 3	Safe	Safe	2.2
C5	-4.73	0.38	Absorbed	54.17	1.25	Non-Inhibitor	Non-Substrate	-1.13	≥ 3	Toxic	Safe	1.43
C6	-4.8	0.249	Absorbed	45.65	0.89	Non-Inhibitor	Non-Substrate	-0.75	≥ 3	Safe	Safe	1.88
C7	-4.86	0.149	Absorbed	43.58	0.68	Non-Inhibitor	Non-Substrate	0.03	≥ 3	Safe	Safe	2.22
C8	-4.79	0.416	Absorbed	56.2	3.56	Non-Inhibitor	Non-Substrate	4.86	≥ 3	Safe	Safe	1.57
C9	-4.71	0.351	Absorbed	29.24	2.48	Non-Inhibitor	Non-Substrate	4.37	≥ 3	Safe	Safe	1.7
C10	-4.81	0.258	Absorbed	46.14	0.89	Non-Inhibitor	Non-Substrate	-0.77	≥ 3	Safe	Safe	1.85
C11	-4.66	0.838	Absorbed	49.53	1.29	Non-Inhibitor	Non-Substrate	15.05	≥ 3	Safe	Toxic	0.17
C12	-4.73	0.828	Absorbed	96.78	1.76	Non-Inhibitor	Substrate	7.38	≥ 3	Safe	Toxic	0.96
C13	-4.8	0.835	Absorbed	Absorbed	1.55	Non-Inhibitor	Substrate	11.62	≥ 3	Safe	Safe	1.86
C14	-4.99	0.847	Absorbed	78.94	2.05	Non-Inhibitor	Substrate	8.75	≥ 3	Safe	Safe	1.08

Caco-2: colon carcinoma cell line permeability; CYP2C9: cytochrome P450 2C9; CYP3A4: cytochrome P450 3A4; F20: probability of oral bioavailability ≥20%; HIA: human intestinal absorption; MTC: maximum tolerated concentration; PPB: plasma protein binding; Vd: volume of distribution

All compounds were predicted to be non-inhibitors of CYP2C9; however, C12, C13, and C14 were identified as CYP3A4 substrates, which may indicate potential metabolic liabilities. Predicted clearance values were highly variable, from negative values in C5 and C10 to high clearance in C11 (15.05 mL/min/kg) and C13 (11.62 mL/min/kg). Despite these differences, all compounds demonstrated half-lives ≥3 h, suggesting sufficient systemic exposure. In terms of toxicity, most compounds were predicted to be non-mutagenic (Ames test: safe) and non-carcinogenic, although exceptions included carcinogenicity alerts in C1, C5, C11, and C12. Maximum tolerated concentration (MTC) values ranged from 0.17 (C11) to 2.22 (C7), with C11 and C12 showing lower thresholds, indicating higher toxicity risk.

Docking with diabetes-associated proteins

The docking study demonstrated that most compounds (C1–C14) exhibited moderate affinities across the five protein targets, generally ranging from −5.0 to −6.5 kcal·mol^{-1}. Stronger binding was observed for several compounds, including C6 (−7.9 kcal·mol^{-1} against PTPN1) and C11 (−6.9 kcal·mol^{-1} against AKR1B1). C12 and C13 were particularly notable, showing consistently high affinities; C12 displayed the strongest binding with α-amylase (−13.6 kcal·mol^{-1}) and NrfA (−8.5 kcal·mol^{-1}), while C13 interacted robustly across all proteins, with binding energies of −9.0 kcal·mol^{-1} (DPP-4), −7.1 kcal·mol^{-1} (PTPN1), −8.1 kcal·mol^{-1} (α-amylase), −9.2 kcal·mol^{-1} (NrfA), and −7.1 kcal·mol^{-1} (AKR1B1). C14 also showed favorable binding, ranging from −6.3 to −8.4 kcal·mol^{-1} (**Table 5**).

Table 5. Docking results for the secondary metabolites of *Melia azedarach* against several diabetes-associated proteins

Compound	Binding affinity (kcal·mol-1)				
	2P8S	2QBP	2QV4	3TOP	4JIR
C1	−5	−5.3	−4.9	−5.2	−5.1
C2	−5.2	−5.6	−5.7	−5.9	−5.2
C3	−5.2	−5.7	−6.1	−6.6	−4.5
C4	−5.4	−5.5	−5.3	−6.3	−5.7
C5	−5.4	−5.8	−5.7	−6.6	−5.2
C6	−5.6	−7.9	−5.7	−6.1	−5.4
C7	−5	−5.8	−5.5	−6.2	−5.1
C8	−5	−5.5	−5.7	−6.5	−4.7
C9	−5.2	−5.2	−5.2	−5.9	−4.6
C10	−4.2	−5.9	−6.2	−6.9	−5.5
C11	−5.5	−5.4	−6.4	−6.5	−6.9
C12	−6.9	−6.5	−13.6	−8.5	−7
C13	−9	−7.1	−8.1	−9.2	−7.1
C14	−8.4	−7.4	−7.1	−7.9	−6.3

Interaction analysis of the best-performing compound, C13, where the visualizations for its interaction with the protein targets are presented in **Figure 3** and **Figure 4**. In DPP-4 (PDB: 2P8S), C13 engaged hydrophobic and hydrogen bond interactions with Phe240, Val252, and Trp124. In PTPN1 (2QBP), important contacts included Lys116 and Phe182. For α-amylase (2QV4), interactions with Pro4 and Asp402 were evident, whereas in NrfA (3TOR), C13 formed stabilizing contacts with Pro1329, Tyr1328, and Gln1406. In AKR1B1 (4JIR), interactions were observed with Lys307, Asp308, and nearby hydrophobic residues such as Leu138 and Ile137.

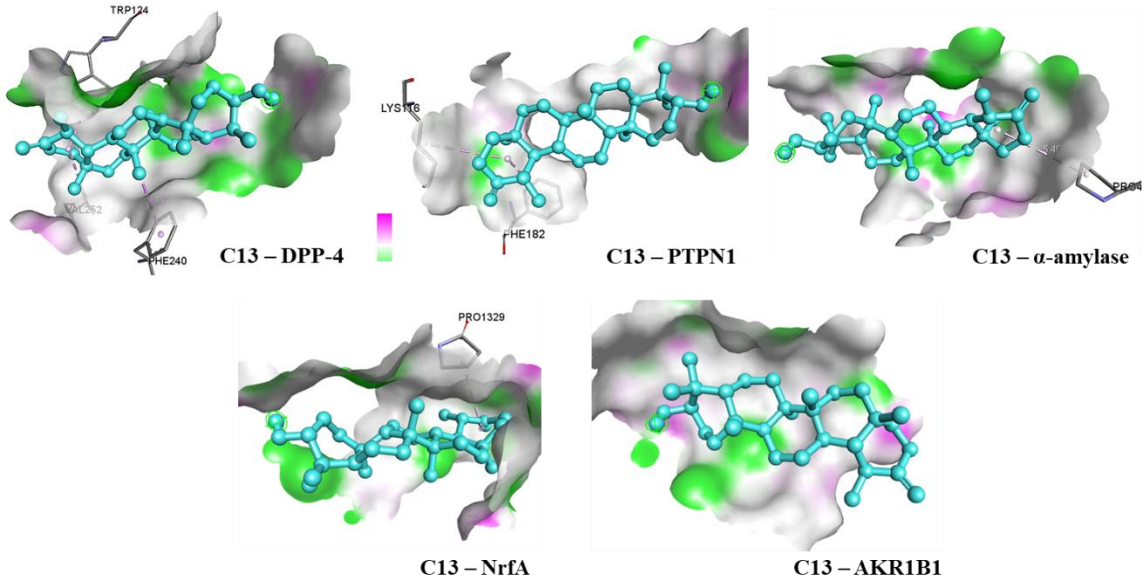

Figure 3. Two-dimensional interaction visualizations of compound C13 docked into the binding pockets of the target proteins.

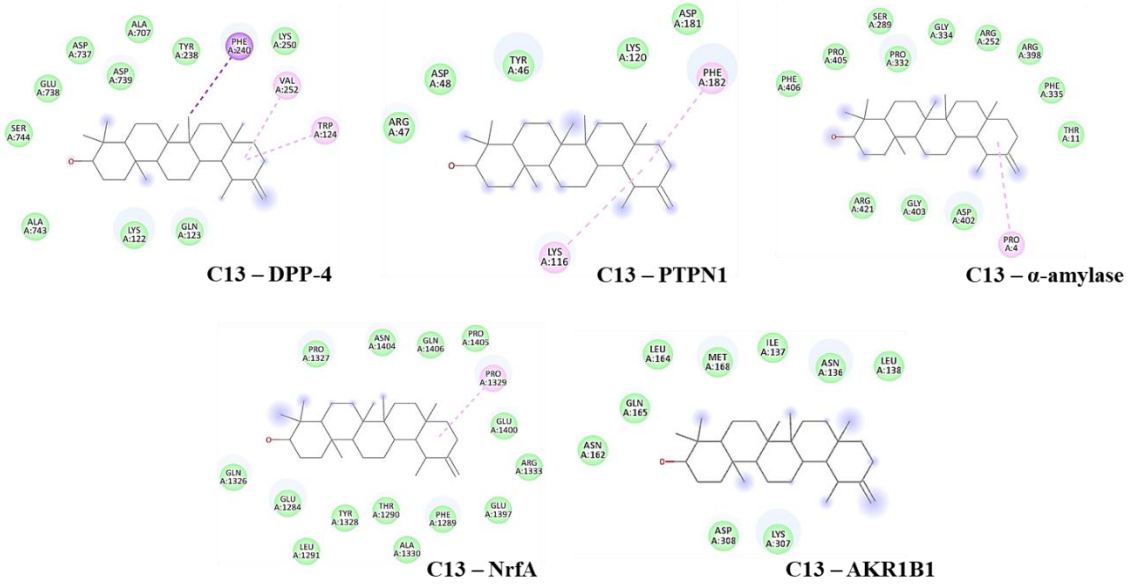

Figure 4. Two-dimensional interaction diagrams of compound C13 docked into the binding pockets of the target proteins

Discussion

Melia azedarach L. has long been recognized in traditional medicine, with its fruits commonly used to manage conditions such as diabetes mellitus, hypercholesterolemia, cancer, and cardiovascular disorders [4,6]. Phytochemical screening of the methanol fruit extract confirmed the presence of terpenoids, flavonoids, and phenolics, consistent with previous reports [25,26]. These bioactive constituents provide a strong rationale for exploring *M. azedarach* fruit as a source of pharmacologically active compounds. Herein, the antioxidant potential of the methanol extract, determined by the DPPH assay, demonstrated a strong free radical scavenging effect (IC_{50} = 102.27 µg/mL). This finding aligns with earlier studies reporting high antioxidant potential in fruit and leaf extracts of *M. azedarach* [27,28]. High total phenolic content (479.8 mg GAE/g) and moderate flavonoid content (52.7 mg QE/g) obtained in the present study further support the role of polar metabolites in driving antioxidant capacity. Terpenoids such as taraxasterol were identified in the extract and are known for their anti-inflammatory, antioxidative, and anticancer

activities [29,30]. Additionally, sesquiterpenes such as himachalene, previously reported to exhibit radical scavenging activity [31], were also detected, broadening the extract's pharmacological relevance.

Following the phytochemical and antioxidant characterization, the present study incorporated in silico ADMET and molecular docking to evaluate drug-likeness and mechanistic potential of selected compounds (C1–C14). The ADMET analysis revealed favorable intestinal absorption and permeability across all compounds. Several compounds demonstrated high plasma protein binding, particularly C12 (96.78%) and C14 (78.94%), suggesting strong systemic retention. Notably, C12, C13, and C14 were predicted as CYP3A4 substrates, raising considerations for metabolic stability, while carcinogenicity alerts were identified for C1, C5, C11, and C12. Clearance predictions varied, with C13 and C11 showing relatively high elimination rates, though all compounds maintained half-lives ≥ 3 h.

Herein, the docking results further highlighted C12, C13, and C14 as lead candidates due to their consistently stronger binding affinities compared with other analogs. C12 exhibited remarkable binding to α-amylase (–13.6 kcal·mol^{-1}), suggesting a potential role in modulating carbohydrate metabolism. This is consistent with reports that cucurbitacins act as α-amylase and α-glucosidase inhibitors and improve glucose metabolism in diabetic models [16,32]. In the present study, C13 displayed broad-spectrum activity, with strong binding across all targets, including DPP-4 (–9.0 kcal·mol^{-1}), PTPN1 (–7.1 kcal·mol^{-1}), and NrfA (–9.2 kcal·mol^{-1}). Interaction mapping confirmed that C13 stabilized within active sites via hydrogen bonding and hydrophobic contacts with residues critical for catalytic function (e.g., Phe240, Val252, Lys116, Asp402, and Lys307). This observation aligns with previous work showing taraxasterol as a dual inhibitor of DPP-4 and PTP1B, capable of improving insulin sensitivity and reducing oxidative stress [33,34]. C14 in the present study also showed favorable docking energies (–6.3 to –8.4 kcal·mol^{-1}), reinforcing its potential as a secondary lead. Stigmastane derivatives, including stigmasta-3,5-diene, have been reported to inhibit α-amylase, α-glucosidase, and PTP1B, as well as exert insulin-sensitizing and glucose-lowering effects in diabetic models [35,36].

This study used only the DPPH assay to assess antioxidant activity, which, while useful for initial screening, does not fully represent the multiple mechanisms of antioxidant defense such as metal chelation, lipid peroxidation inhibition, or cellular ROS scavenging. The ADMET profiling and docking evaluations were entirely in silico, providing predictive insights but lacking experimental pharmacokinetic and toxicological validation. In addition, only a subset of compounds identified from the extract were computationally analyzed, leaving other potentially active metabolites untested. These limitations highlight the need for complementary antioxidant assays, in vivo pharmacological studies, molecular dynamics simulations, and comprehensive toxicity testing to confirm the therapeutic promise of *M. azedarach* compounds.

Conclusion

Our study revealed that *M. azedarach* fruit extract is a promising source of antioxidant and bioactive compounds with potential applications in metabolic disorders, particularly diabetes mellitus. The integration of antioxidant profiling, ADMET predictions, and docking analysis highlights the cucurbitacin compound and taraxasterol as strong candidates, although safety concerns (e.g., CYP3A4 metabolism and carcinogenicity alerts) require further toxicological validation. These results not only support the ethnomedicinal use of *M. azedarach* but also provide a scientific basis for its development into novel therapeutic agents.

Ethics approval

None to declare.

Acknowledgments

None to declare.

Competing interests

All the authors declare that there are no conflicts of interest.

Funding

This study received no external funding.

Underlying data

Derived data supporting the findings of this study are available from the corresponding author on request.

Declaration of artificial intelligence use

This work used artificial intelligence (AI) tools and methodologies in manuscript writing support. ChatGPT was employed to language refinement and technical writing assistance. We confirm that all AI-assisted processes were critically reviewed by the authors to ensure the integrity and reliability of the results. The final decisions and interpretations presented in this article were solely made by the authors.

How to cite

Aini Q, Nurdin N, Mustanir M, *et al*. Phytochemical screening of bioactive compounds and antioxidant activity of methanol extract from *Melia Azedarach* L. fruit: Exploring for antidiabetic potential. Narra X 2025; 3 (2): e229 - http://doi.org/10.52225/narrax.v3i2.229.

References

1. Priyono DS, Sofyantoro F, Putri WA, *et al*. A bibliometric analysis of Indonesia biodiversity identification through DNA barcoding research from 2004-2021. Nat Life Sci Commun 2023;22(1):e2023006.
2. Arunachalam A, Sahoo UK, Upadhyaya K. Exploring research trends and priorities of genus Melia. Sci Rep 2024;14(1):6265.
3. Doudi M, Rasnovi S, Dahlan D, *et al*. Study of medicinal plants in the geothermal area of Mount Seulawah Agam, Aceh Besar District, Indonesia. J Natural 2021;21(3):114-122.
4. Kar D, Ghosh P, Suresh P, *et al*. Review on phyto-chemistry & pharmacological activity of *Melia azedarach*. Int J Exp Res Rev 2022;28:38-46.
5. Song M, Luo H-J, Li Z-W, *et al*. Limonoids from the roots of *Melia azedarach* and their anti-inflammatory activity. Phytochemistry 2023;216:113869.
6. Cao F, Chen J, Lin Z-T, *et al*. Chemical constituents from the fruit of *Melia azedarach* and their anti-inflammatory activity. Antioxidants 2024;13(11):1338.
7. Ong KL, Stafford LK, McLaughlin SA, *et al*. Global, regional, and national burden of diabetes from 1990 to 2021, with projections of prevalence to 2050: a systematic analysis for the Global Burden of Disease Study 2021. The Lancet 2023;402(10397):203-234.
8. Natalie J, Gondokesumo ME, Wahjudi M. Indonesian medicinal plants as potential candidates for alpha-glucosidase inhibitor: A comprehensive literature review for anti-diabetic therapy. J Teknol Laboratorium 2025;14(2):124-128.
9. Ismail M, Rahman A, Umar M, *et al*. Anti-diabetic and Anti-Inflammatory activities of *Melia azedarach* extract. Phytopharmacol Res J 2024;3(2):44-48.
10. Seifu D, Gustafsson LE, Chawla R, *et al*. Antidiabetic and gastric emptying inhibitory effect of herbal *Melia azedarach* leaf extract in rodent models of diabetes type 2 mellitus. J Exp Pharmacol 2017;9:23-29.
11. Khan MF, Rawat AK, Khatoon S, *et al*. In vitro and in vivo antidiabetic effect of extracts of *Melia azedarach*, *Zanthoxylum alatum*, and *Tanacetum nubigenum*. Integr Med Res 2018;7(2):176-183.
12. Saini K, Sharma S, Khan Y. DPP-4 inhibitors for treating T2DM-hype or hope? an analysis based on the current literature. Front Mol Biosci 2023;10:1130625.
13. Stein V, Geserick P, Friedrich K, *et al*. Pro-inflammatory cytokines as regulators of protein tyrosine phosphatases and insulin signaling in murine skeletal muscle cells. Cell Signal 2025:112037.
14. Teimouri M, Hosseini H, ArabSadeghabadi Z, *et al*. The role of protein tyrosine phosphatase 1B (PTP1B) in the pathogenesis of type 2 diabetes mellitus and its complications. J Physiol Biochem 2022;78(2):307-322.
15. Kaur N, Kumar V, Nayak SK, *et al*. Alpha-amylase as molecular target for treatment of diabetes mellitus: A comprehensive review. Chem Biology Drug Des 2021;98(4):539-560.
16. Kashtoh H, Baek K-H. New insights into the latest advancement in α-amylase inhibitors of plant origin with anti-diabetic effects. Plants 2023;12(16):2944.

17. Al-Hussan R, Albadr NA, Alshammari GM, *et al*. Phloretamide prevent hepatic and pancreatic damage in diabetic male rats by modulating Nrf2 and NF-κB. Nutrients 2023;15(6):1456.
18. Kaur N, Vanita V. Association of aldose reductase gene (AKR1B1) polymorphism with diabetic retinopathy. Diabetes Res Clin Pract 2016;121:41-48.
19. Zheng X-Z, Yu H-Y, Chen Y-R, Fang J-S. Aucubin mitigates the elevation of microglial aerobic glycolysis and inflammation in diabetic neuropathic pain via aldose reductase. World J Diabetes 2025;16(5):103915.
20. Yahya M, Ginting B, Saidi N. In-vitro screenings for biological and antioxidant activities of water extract from *Theobroma cacao* L. Pod husk: Potential utilization in foods. Molecules 2021;26(22):6915.
21. Sitohang NA, Putra ED, Kamil H, Musman M. Acceleration of wound healing by topical application of gel formulation of *Barringtonia racemosa* (L.) Spreng kernel extract. F1000Research 2022;11:191.
22. Iwansyah AC, Desnilasari D, Agustina W, *et al*. Evaluation on the physicochemical properties and mineral contents of *Averrhoa bilimbi* L. leaves dried extract and its antioxidant and antibacterial capacities. Food Sci Technol 2021;41:987-992.
23. Masjedi M, Nateghi L, Berenjy S, Eshaghi MR. Optimization of extraction of flavonoid, total phenolic, antioxidant, and antimicrobial compounds from *Ganoderma lucidum* by maceration method. Iran J Chem Chem Eng 2022;41(9):3127-3140.
24. Ginting B, Yahya M, Saidi N, *et al*. Antioxidant and cytotoxicity screenings of ethyl acetate extract from *Annona muricata* leaves and its fractions. J Adv Pharm Technol Res 2024;15(2):70-74.
25. Malar TJ, Antonyswamy J, Vijayaraghavan P, *et al*. In-vitro phytochemical and pharmacological bio-efficacy studies on *Azadirachta indica* A. Juss and *Melia azedarach* Linn for anticancer activity. Saudi J Biol Sci 2020;27(2):682-688.
26. Farook M, Mohamed H, Tariq N, *et al*. Phytochemical screening, antibacterial and antioxidant activity of *Melia azedarach*. Int J Res Anal Rev 2019;6(2):248-255.
27. Muzafar W, Kanwal T, Rehman K, *et al*. Green synthesis of iron oxide nanoparticles using *Melia azedarach* flowers extract and evaluation of their antimicrobial and antioxidant activities. J Mol Struct 2022;1269:133824.
28. Azhar F, Latif A, Rafay MZ, *et al*. Preliminary Studies and In-vitro Antioxidant Activity of Fruit-Seed Extracts of *Melia azedarach* Linn. Int J Inn Sci Res Technol 2022;7(1):1328-1335.
29. Obafemi OT, Ayeleso AO, Obafemi BA, *et al*. Pharmacological relevance of taraxasterol: A review. Pharmacol Res Mod Chin Med 2024;13:100533.
30. Wang C-Y, Chen Y-W, Hou C-Y. Antioxidant and antibacterial activity of seven predominant terpenoids. Int J Food Prop 2019;22(1):230-238.
31. Jaouadi I, Cherrad S, Bouyahya A, *et al*. Chemical variability and antioxidant activity of *Cedrus atlantica* Manetti essential oils isolated from wood tar and sawdust. Arab J Chem 2021;14(12):103441.
32. Anitha T, Balamurugan V, Kabilan M, *et al*. Cucurbits as a natural pharmacy: A review of phytochemical richness and therapeutic potentials. Ann Phytomed 2025;14(1):314-326.
33. Zhao M, Lu M, Zeng Y, *et al*. Taraxasterol inhibits hepatic gluconeogenesis and increases glycogen synthesis via the PI3K/Akt signaling pathway. Nat Prod Commun 2023;18(3):1934578X231154068.
34. Ogunyemi OM, Gyebi GA, Olawale F, *et al*. Identification of promising dipeptidyl peptidase-4 and protein tyrosine phosphatase 1B inhibitors from selected terpenoids through molecular modeling. Bioinform Adv 2025;5(1):vbae205.
35. Lolok N, Ramadhan D, Sumiwi S, *et al*. Molecular docking of β-Sitosterol and stigmasterol isolated from Morinda citrifolia with α-amylase, α-glucosidase, dipeptidylpeptidase-IV, and peroxisome proliferator-activated receptor-γ. Rasayan J Chem 2022;15(1):20.
36. Salehi B, Quispe C, Sharifi-Rad J, *et al*. Phytosterols: From preclinical evidence to potential clinical applications. Front Pharmacol 2021;11:599959.